Circuit Modeling of Carrier–Photon Dynamics in Composite-Resonator Vertical-Cavity Lasers

Bhavin J. Shastri, *Student Member, IEEE*, Chen Chen, *Member, IEEE*, Kent D. Choquette, *Fellow, IEEE*, and David V. Plant, *Fellow, IEEE*

Abstract

recombination, $_{gk}$ is the group velocity of the optical mode in the lasing medium, λ_k is the percentage of the optical standing wave overlapping with the respective cavity, $_{p}$ is the photon lifetime, $_{k}$

where

$$I_k^{T1} = I_k^{D1} + I_k^{C1} \tag{19}$$

$$I_k^{T2} = I_k^{D2} + I_k^{C2} \tag{20}$$

$$I_k^{D1} = \frac{q N_{k0} V_{\text{act}k}}{2\eta_{ik\ k}} \left[\exp\left(\frac{qV_k}{nkT}\right) - 1 \right] \tag{21}$$

$$I_k^{D2} = \frac{q N_{k0} V_{\text{act}k}}{2\eta_{ik\ k}} \left[\exp\left(\frac{qV_k}{nkT}\right) - 1 + \frac{2q\ _k}{nkT} \exp\left(\frac{qV_k}{nkT}\right) \frac{dV_k}{dt} \right] \tag{22}$$

$$I_k^{C1} = I_k^{C2} = \frac{q N_{k0} V_{\text{act}k}}{2\eta_{ik\ k}} \tag{23}$$

$$B_k^N = \frac{\lambda\ _p q\ _{gk\ k}}{\eta_{ik}\eta_c hc} \frac{g\left(\ _k I_k^{T1}\right)}{_k\left(\ \cdot\ V_m + \delta^{\ 2}\right)}\ V_m + \delta^{\ 2} \times \left[1 + \left(\frac{\blacklozenge_1 V_{\text{act}1}}{\blacklozenge_2 V_{\text{act}2}} \right)^{-1\ _k} \right]^{-1} \tag{24}$$

with

$$_k = \frac{2\eta_{ik\ k}}{q V_{\text{act}k}} \quad \text{and} \quad N_k = \ _k I_k^{T1} \tag{25}$$

Similarly, to model the photon dynamics $dS\ dt$, we substitute the transformations (15) and (16) and the output power (8), into the rate equations (3). After applying appropriate manipulations, we obtain

$$2\ V_m + \delta\ \frac{dV_m}{dt} = -\frac{V_m + \delta^{\ 2}}{p} + \frac{\beta_1 N_1}{_1} + \frac{\beta_2 N_2}{_2} + \left\{ \ _1\ g1\blacklozenge_1 \frac{g\ \ N_1}{_1\left(\ \ V_m + \delta^{\ 2}\right)} + \ _2\ g2\blacklozenge_2 \frac{g\ \ N_2}{_2\left(\ \ V_m + \delta^{\ 2}\right)} \right\}\ V_m + \delta^{\ 2} \tag{26}$$

With some additional rearrangements and the definition of suitable circuit elements, (26) can be rewritten as

$$C_{ph} \frac{dV_m}{dt}$$

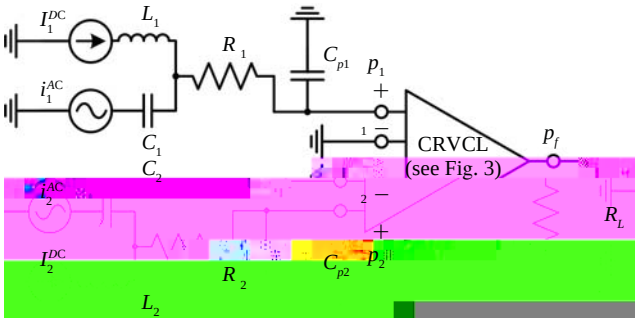

Fig. 4. Circuit setup to simulate the CRVCL equivalent circuit model.

TABLE I
CRVCL DEVICE PARAMETERS USED IN EQUIVALENT CIRCUIT MODEL [5], [8], [15], [17]

	D	
η_1 η_2	Current-injection efficiency	0.86
λ	Lasing wavelength	850 nm
V_{act1}	Top cavity active region volume	1.2×10^{-18} m^3
V_{act2}	Bottom cavity active region volume	2.4×10^{-18} m^3
1 2	Optical confinement factor	0.055
$g1$ $g2$	Lasing medium group velocity	3 3.5×10^{10} cm s
	Optical standing wave overlap factor	0.5
1 2	Carrier lifetime	2.6 ns
p	Photon lifetime	2.5 ps
g_{10} g_{20}	10	

$$\left|\frac{s}{j_1}\right| = \left|\frac{{}_1 \; {}_1g_1'S_0 \;\; qd_1}{{}^2 + i \quad 1 \quad {}_1 + \; {}_1g_1'\lambda_t S_0 \; - \; {}_1^2 \; {}_1\lambda_t g_{10}g_1'S_0 - \; {}_2^2 \; {}_2\lambda_t g_{20}g_2'S_0\gamma}\right| \tag{32}$$

$$\gamma = \frac{i \quad - \; 1 \quad {}_1 + \; {}_1g_1'\lambda_t S_0}{i \quad - \; 1 \quad {}_2 + \; {}_2g_2'\lambda_t S_0} \tag{33}$$

$$\left|\frac{s}{j_2}\right| = \left|\frac{{}_2 \; {}_2g_2'S_0 \;\; qd_2}{{}^2 + i \quad 1 \quad {}_2 + \; {}_2g_2'\lambda_t S_0 \; - \; {}_2^2 \; {}_2\lambda_t g_{20}g_2'S_0 - \; {}_1^2 \; {}_1\lambda_t g_{10}g_1'S_0 \;\; \gamma}\right| \tag{34}$$

above the RO frequency including the RC bandwidth, they do not compare well for frequencies below the RO frequency. This is not the case with the proposed circuit model where the results are comparable across all frequencies. It should be noted that the analytical model solves the rate equations algebraically obtaining a closed-form expression, whereas the circuit model solves the rate equations numerically by accounting for the interdependence between laser parameters. The proposed circuit model provides an improvement over the existing analytical model.

2) Cavity Detuning Characteristics: Fig. 7(a) shows the simulated CRVCL circuit model modulation response as a function of the percentage of the optical longitudinal mode overlapping with the top cavity (λ_t), when only the top cavity is under direct modulation. The simulations depicted in Fig. 7(a) only vary (λ_t) and assume the other cavity parameters are the same for both cavities. Although different optical field distribution may lead to changes in other cavity parameters, such as the gain coefficient and differential gain, the proposed equivalent CRVCL circuit model use these simplified assumptions. It can be observed from Fig. 7(a) that the modulation response has an increasing RO peak and greater modulation bandwidth as more optical field is confined in the top cavity. On the other hand, Fig. 7(b) shows the CRVCL modulation response as a function of λ_t, when only the bottom cavity is under direct modulation. Similarly, the modulation response can be engineered by varying the detuning between both cavities. However, it is interesting to observe that the modulation response exhibits the opposite trend as compared to Fig. 7(a).

The case when $\lambda_t = 50\%$ in Figs. 7(a) and 7(b) correspond to the same modulation response, which is also equivalent to the modulation response of a conventional VCSEL with the same photon density. When more optical field is confined in the top cavity, the modulation response becomes more damped (decreasing RO peak) and the modulation bandwidth decreases. Therefore, for a given λ_t, we can obtain two different modulation responses, depending on which cavity we have chosen to apply direct modulation. For an appropriate λ_t, the CRVCL would achieve a larger bandwidth than that of a conventional VCSEL with the same photon density. This is

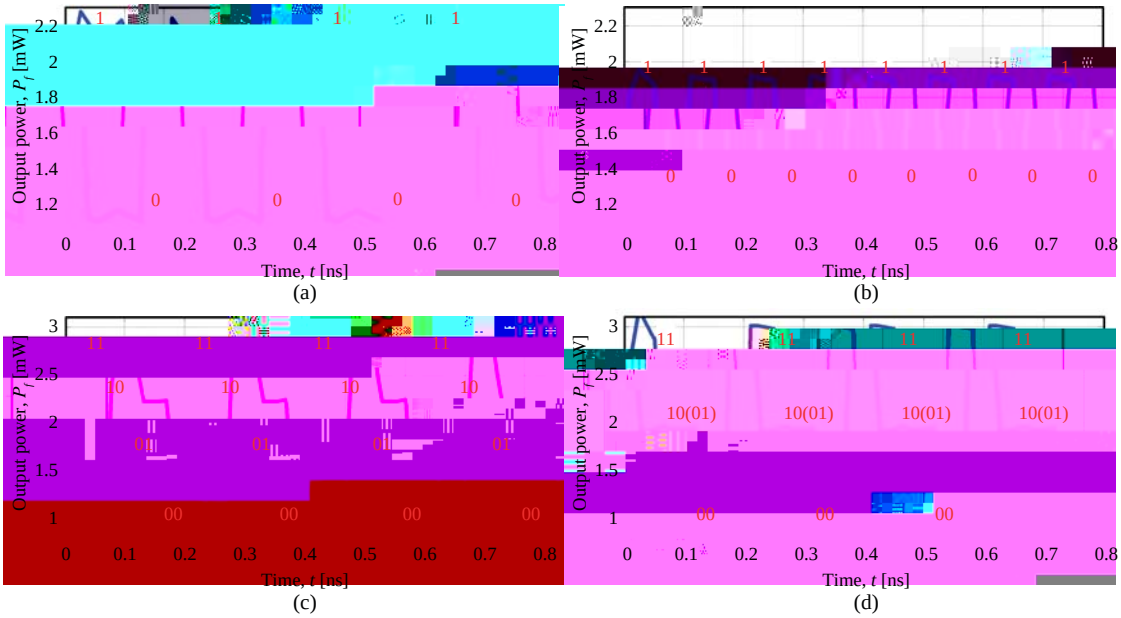

Fig. 8. Circuit modeling of optical output signal when only the (a) top cavity and (b) botto

mode, another photon equation needs to be added and the electrical carrier equations (1) and (2) need to be modified so that the carriers are consumed by two simulated emission processes; we also need to consider the cross terms such as the cross gain compression and phase detuning of two longitudinal modes. Due to the additional interdependence between photons and carriers interactions, the rate equations can be only solved using numerical methods such as the Runge-Kutta method [15]. In this paper, we show that by mapping the CRCVL rate equations into a circuit model, SPICE analysis can be used as an efficient and accurate implementation of numerical calculations. And we believe that this circuit approach would also provide a smooth upgrade when more complex higher-order CRVCL effects are incorporated in the future. Nevertheless, the current circuit model will still be useful when a predominant single longitudinal mode is desired for applications such as push-pull modulation [8]. This single longitudinal mode condition can be achieved by setting a proper cavity detuning and/or gain/cavity spectral alignment.

In addition, we have verified that using the proposed circuit model, the asymmetries between the coupled cavities can be used to engineer the CRCVL modulation response. We also confirm the CRVCL's uniI.7(e)2odgal00.5(d3o)-7.o5(d3o)-7